



# Association of Tau Pathology With Clinical Symptoms in the Subfields of Hippocampal Formation

## OPEN ACCESS

### Edited by:

Rong Chen,  
University of Maryland, Baltimore,  
United States

### Reviewed by:

Muthuswamy Anusuyadevi,  
Bharathidasan University, India  
Gabriel Gonzalez-Escamilla,  
Johannes Gutenberg University  
Mainz, Germany

### \*Correspondence:

Junhai Xu  
jhxu@tju.edu.cn  
Yuanjie Zheng  
yjzheng@sdnu.edu.cn

† These authors have contributed  
equally to this work

\*\* Data used in preparation of this  
article were partly obtained from the  
Alzheimer's Disease Neuroimaging  
Initiative (ADNI) database  
(adni.loni.usc.edu). As such, the  
investigators within the ADNI  
contributed to the design and  
implementation of ADNI and/or  
provided data but did not participate  
in analysis or writing of this report. A  
complete listing of ADNI investigators  
can be found at: [http://adni.loni.usc.edu/wp-content/uploads/how\\_to\\_apply/ADNI\\_Acknowledgement\\_List.pdf](http://adni.loni.usc.edu/wp-content/uploads/how_to_apply/ADNI_Acknowledgement_List.pdf)

**Received:** 25 February 2021

**Accepted:** 20 May 2021

**Published:** 14 July 2021

### Citation:

Ge X, Zhang D, Qiao Y, Zhang J, Xu J  
and Zheng Y (2021) Association of  
Tau Pathology With Clinical  
Symptoms in the Subfields of  
Hippocampal Formation.  
*Front. Aging Neurosci.* 13:672077.  
doi: 10.3389/fnagi.2021.672077

Xinting Ge<sup>1,2,3†</sup>, Dan Zhang<sup>2†</sup>, Yuchuan Qiao<sup>2</sup>, Jiong Zhang<sup>2</sup>, Junhai Xu<sup>4\*</sup> and Yuanjie Zheng<sup>1\*</sup> on behalf of Alzheimer's Disease Neuroimaging Initiative\*\*

<sup>1</sup>School of Information Science and Engineering, Shandong Normal University, Jinan, China, <sup>2</sup>Laboratory of Neuro Imaging (LONI), USC Stevens Neuroimaging and Informatics Institute, Keck School of Medicine, University of Southern California, Los Angeles, CA, United States, <sup>3</sup>School of Medical Imaging, Xuzhou Medical University, Xuzhou, China, <sup>4</sup>College of Intelligence and Computing, Tianjin Key Lab of Cognitive Computing and Application, Tianjin University, Tianjin, China

**Objective:** To delineate the relationship between clinical symptoms and tauopathy of the hippocampal subfields under different amyloid statuses.

**Methods:** One hundred and forty-three subjects were obtained from the ADNI project, including 87 individuals with normal cognition, 46 with mild cognitive impairment, and 10 with Alzheimer's disease (AD). All subjects underwent the tau PET, amyloid PET, T1W, and high-resolution T2W scans. Clinical symptoms were assessed by the Neuropsychiatric Inventory (NPI) total score and Alzheimer's Disease Assessment Scale cognition 13 (ADAS-cog-13) total score, comprising memory and executive function scores. The hippocampal subfields including Cornu Ammonis (CA1–3), subiculum (Sub), and dentate gyrus (DG), as well as the adjacent para-hippocampus (PHC) and entorhinal cortex (ERC), were segmented automatically using the Automatic Segmentation of Hippocampal Subfields (ASHS) software. The relationship between tauopathy/volume of the hippocampal subfields and assessment scores was calculated using partial correlation analysis under different amyloid status, by controlling age, gender, education, apolipoprotein E (APOE) allele  $\epsilon$ 4 carrier status, and, time interval between the acquisition time of tau PET and amyloid PET scans.

**Results:** Compared with amyloid negative (A–) group, individuals from amyloid positive (A+) group are more impaired based on the Mini-mental State Examination (MMSE;  $p = 3.82e-05$ ), memory ( $p = 6.30e-04$ ), executive function ( $p = 0.0016$ ), and ADAS-cog-13 scores ( $p = 5.11e-04$ ). Significant decrease of volume (CA1, DG, and Sub) and increase of tau deposition (CA1, Sub, ERC, and PHC) of the hippocampal subfields of both hemispheres were observed for the A+ group compared to the A- group. Tauopathy of ERC is significantly associated with memory score for the A- group, and the associated regions spread into Sub and PHC for the A+ group. The relationship between the impairment of behavior or executive function and tauopathy of the hippocampal subfield was discovered within the A+ group. Leftward asymmetry was observed with the association between assessment scores and tauopathy of the hippocampal subfield, which is more prominent for the NPI score for the A+ group.

**Conclusion:** The associations of tauopathy/volume of the hippocampal subfields with clinical symptoms provide additional insight into the understanding of local changes of the human HF during the AD continuum and can be used as a reference for future studies.

**Keywords:** Alzheimer's disease, hippocampal subfield, tau pathology, PET imaging, behavior symptoms

## INTRODUCTION

Alzheimer's disease (AD) is characterized by the deposition of pathologic amyloid and tau proteins (Marks et al., 2017; Gordon et al., 2019; Scharre, 2019). Compared with  $\beta$ -amyloid ( $A\beta$ ) plaques, tau deposition has been found to have a stronger association with cognitive decline during the AD continuum (Brier et al., 2016). Specimen research has revealed that the arise of tau deposition is firstly found in the trans-entorhinal cortex and then spreads into the temporal lobe regions such as the hippocampal formation (HF), and finally reaches the neocortex (Braak and Del Tredici, 2011; Braak et al., 2011). As the central node of the mnemonic circuitry, impairment of the HF has received much attention from other researchers (Yushkevich et al., 2015; Adler et al., 2018; Evans et al., 2018) to study the occurrence and progression of AD.

The HF has been associated with memory and cognitive functions and is conventionally used as one of the early biomarkers of several neuropsychiatric disorders including AD and Parkinson's disease (PD; Ikram et al., 2010; Adler et al., 2018; Das et al., 2019). AD subjects present a significant decrease in hippocampal volume and multifaceted impairment of adult hippocampal neurogenesis (AHN) compared to cognitively normal (CN) individuals (Adler et al., 2018; Moreno-Jiménez et al., 2019). However, morphometry changes of the whole HF may be insufficient to delineate the detailed neurodegenerative features during the progression of AD as the human HF is comprised of several substructures including the dentate gyrus (DG), the Cornu Ammonis (CA), the subiculum (Sub), and the associated white matter tracts (Naidich et al., 1987). Subfields of the HF may exhibit differential patterns in their association with cognitive performance in specific domains, as well as the subsequent risk of dementia. The atrophy of subiculum and pre-subiculum regions were found strongly associated with executive dysfunction (Evans et al., 2018). CA1 and fimbria also showed the trend toward significant volume reduction with the progression of AD (Parker et al., 2019; Zhao et al., 2019). In addition, the impairment of the HF can be regarded as the neurodegeneration assessment following the amyloid/tau/neurodegeneration (AT[N]) framework (Jack et al., 2016, 2019; Jack Jr et al., 2018). The spreading patterns of biomarker findings such as tau deposition of the hippocampal subfields, as well as its association with the clinical symptoms during the AD continuum, however, remain relatively underexplored.

In addition, behavioral changes are the accompanying characteristics with AD progression and severely impact the

patients' quality of life and caregivers' burdens (Zhao et al., 2016; Deb et al., 2018). CN individuals with abnormal behavior symptoms were found to be at higher risk of developing mild cognitive impairment (MCI; Mok et al., 2004; Masters et al., 2015). Much research has demonstrated that the presence of mild behavioral impairment can be used as an "at-risk" state for cognitive decline and dementia (Ismail et al., 2016; Yoon et al., 2019). As one of the early markers of AD, impairment of the hippocampal subfield may also be associated with the rise of behavior symptoms. The characterization of these relationships will help us to determine if the presence of behavior symptoms provides additional information for the understanding of the AD continuum.

The specific aim of the current study was to observe the relationship between tau deposition of each hippocampal subfield and clinical symptoms (assessed by the memory, cognition, executive function, and behavior scores) under different amyloid status (amyloid negative and positive). The Alzheimer's Disease Assessment Scale-Cognitive (ADAS-cog) was used to measure the cognitive performance (Petersen et al., 2010; Kueper et al., 2018) and the Neuropsychiatric Inventory (NPI) was used to quantify the severity and frequency of behavior symptoms in the ADNI project (Cummings, 1997; Nunes et al., 2019). The volume of each hippocampal subfield was also assessed in the current research to calculate its association with the clinical scores. AD-related factors including age, gender, education, and apolipoprotein E (APOE) allele  $\epsilon 4$  carrier status were considered in the statistical analysis based on previous studies (Tosun et al., 2017; McCartney et al., 2018). We hypothesize that the tauopathy/volume of different hippocampal subfields may have diverse association patterns with the clinical symptoms, even under the same amyloid status. They may exhibit an enhanced association between the tauopathy/volume of hippocampal subfield and the clinical symptoms with the presence of amyloid pathology. Our results may provide additional insight into the detailed analysis of the local changes of the human HF during the AD continuum and can be used as the reference for future AD studies.

## MATERIALS AND METHODS

### Participant

ADNI project was conducted to measure the progression of MCI and early AD based on serial MRI, PET, other biomarkers, and clinical and neuropsychological assessments (Weiner et al., 2015). The diagnostic criteria in ADNI was described beforehand and informed written consent was obtained from all participants

**TABLE 1** | Data characteristics (A–: amyloid negative, A+ : amyloid positive, n.s.: no significant,  $p < 0.05$ ).

Amyloid status	A–	A+	P-value
Number of subjects (N)	88	55	
CN/MCI/AD	59/28/1	28/18/9	
Age (years)	75.05 ± 6.77	77.99 ± 7.90	0.0192
Education (years)	16.40 ± 2.68	16.47 ± 2.73	n.s.
Gender (M/F)	40/48	24/31	n.s.
APOE $\epsilon$ 4 (0/1/2)	71/15/1	25/22/7	1.96e-06
MMSE	28.75 ± 1.74	26.55 ± 4.35	3.82e-05
Memory	0.82 ± 0.69	0.31 ± 0.98	6.30e-04
Executive function	0.94 ± 0.95	0.33 ± 1.24	0.0016
ADAS-cog-13	14.23 ± 6.02	19.58 ± 10.10	1.33e-04
NPI	2.86 ± 6.40	5.07 ± 8.94	n.s.

at each site (Petersen et al., 2010). In our study, we firstly screened subjects who underwent both  $^{18}\text{F}$ -AV-1451 PET and structural T1 scans in the latest visit. Subjects with amyloid florbetapir (AV-45) PET scans and T2 scans (High-resolution hippocampus sequence) within the time interval of 1 year before/after the acquisition time of tau PET scans were then selected. The A $\beta$  status was determined by previous studies with a cutoff of 1.11 for AV-45 tracer (Landau et al., 2014). Participants with age >65 years and complete cognitive and behavioral assessments were included in our study as we focused on late-onset AD. By June 11th of 2019, 143 participants meeting the above requirements were selected from ADNI-2 and ADNI-3 (Table 1).

## T1-Weighted and T2-Weighted MRI Acquisition and Processing

All subjects were scanned by 3.0 T MRI scanners using a 3D MP-RAGE or IR-SPGR T1-weighted sequences and high-resolution hippocampus T2-weighted sequence. The detailed protocol can be found online<sup>1</sup>.

## Tau PET Image Acquisition and Processing

Tau PET images were preprocessed according to the standardized protocols at each ADNI site. All images were verified with quality control and processed with realignment, averaging, and resampled to an isotropic voxel size of 8 mm. We obtained the brain ROIs based on the Desikan-Killiany Atlas (Desikan et al., 2006) and mapped the PET image to the structural T1-weighted MRI image. Standardized uptake value ratio (SUVR) images were calculated for each subject using the whole cerebellum gray matter as the reference region.

## Segmentation of the Hippocampal Subfields

ASHS (Automatic Segmentation of Hippocampal Subfields) software was used for the automatic segmentation of the hippocampal subfields for each subject<sup>2</sup>. T1 weighted and high-resolution T2 weighted MRI data were imported into the ASHS to automatically parcellate the HF and adjacent brain regions into CA1, CA2, CA3, Sub, para-hippocampus (PHC),

entorhinal cortex (ERC), and DG (Figure 1). The ERC and PHC were also considered in the current study as these two regions were adjacent to the HF and were closely related to the progression of AD. The CA2 and CA3 regions were considered together in the following analysis as the size of these regions were relatively small. Mean SUVRs of the six regions on each hemisphere were finally calculated from the SUVR images.

## Clinical Symptoms

In the current research, we focus on the behavior score and the cognition score, as well as the comprised memory and executive function scores to delineate their relationship with tau pathology. The total score of NPI based on 12 domains was used to assess the behavioral symptoms. The total score of ADAS-cog based on 13 domains was used to measure cognitive symptoms. The composite score for memory was composed of scores of the Rey's Auditory Vocabulary List Test (RAVLT), Alzheimer's Disease Assessment Scale—cognitive subscale-11 (ADAS-Cog), Logical Memory (LM), and MMSE recall scores. The composite score for executive function included Category Fluency (animals and vegetables scores), Trail Making Test (TMT) A and B, Digit span backward, Wechsler Adult Intelligence Scale-Revised (WAIS-R) Digit Symbol Substitution, and five Clock drawing items (circle, symbol, numbers, hands, time). Clinical scores were acquired within the time interval of 3 months before/after the acquisition time of Tau PET scans.

## Statistical Analysis

For paired group comparison based on amyloid status (A+ and A–), a two-tailed Student *t*-test was applied to the mean SUVR or volume of each hippocampal subfield between A– and A+ groups. For hemispheric comparison, a two-tailed Student *t*-test was applied to the mean SUVR or volume of each hippocampal subfield between the left and right hemisphere under different amyloid status.

To assess the association of clinical symptoms and mean SUVR (or volume) of each hippocampal subfield, partial correlation analysis was conducted on two groups (A+ and A–) for each hippocampal subfield. The NPI total score, ADAS-cog-13 total score, comprised memory score, and comprised executive function score were treated as the response variable and the mean SUVR or volume of each hippocampal subfield as the predictor. Age, gender, education, APOE allele  $\epsilon$ 4 carrier status, and the time interval between the acquisition time of amyloid PET and tau PET scans were used as the covariates of the partial correlation analysis. For all statistical tests, the false discovery rate (FDR) correction was applied for the correction of multiple comparisons. An adjusted *p*-value less than 0.05 was considered as statistically significant in all analyses.

## Data Availability

All ADNI data used in our experiments are publicly available through LONI IDA<sup>3</sup>.

<sup>1</sup><http://adni.loni.usc.edu/methods/documents/mri-protocols>

<sup>2</sup><http://picl.upenn.edu/software/ashs/>

<sup>3</sup><https://ida.loni.usc.edu/>

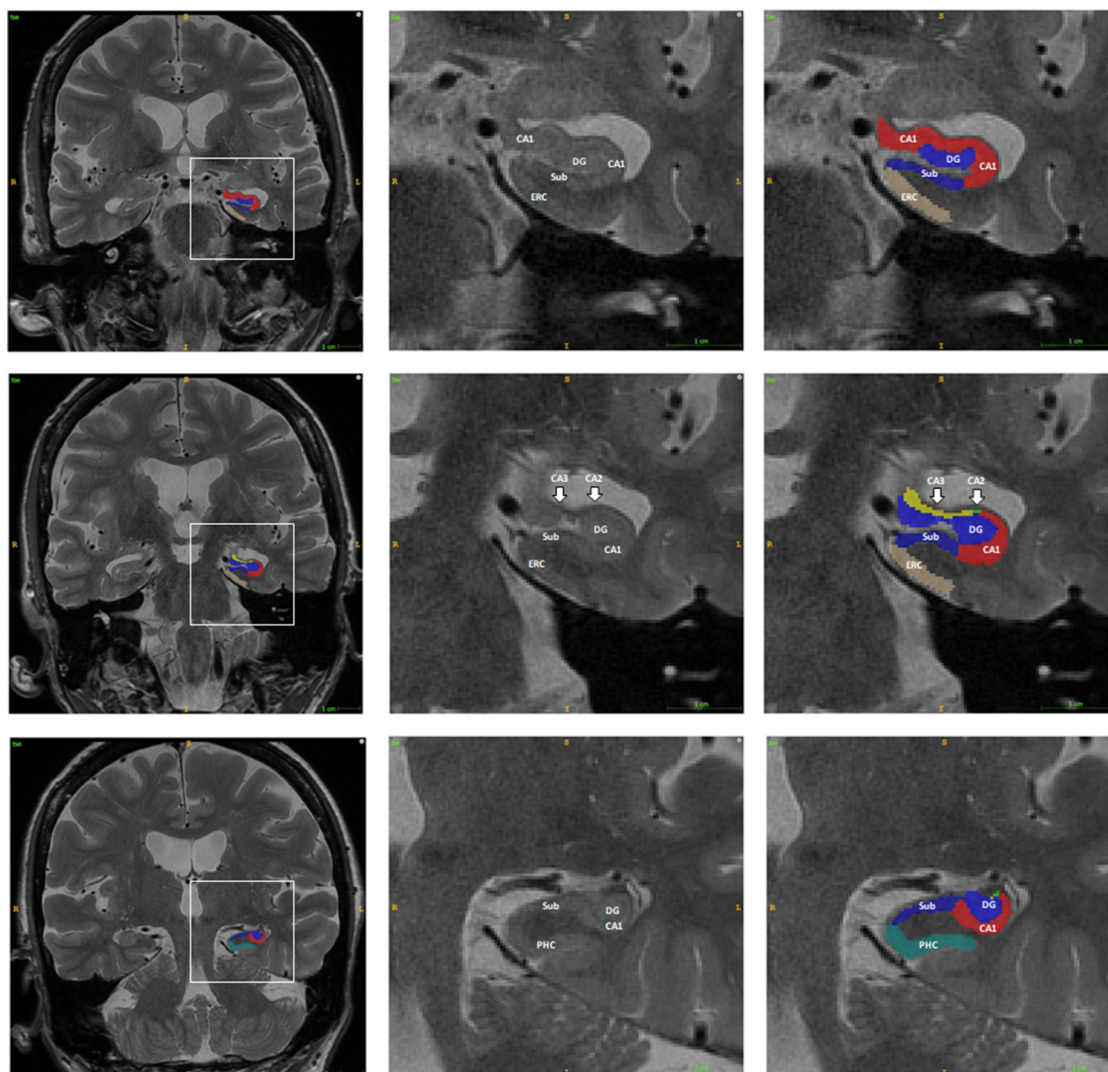


**FIGURE 1** | Example of the automatic segmentation of the hippocampal subfield using ASHS software. The boundary of each hippocampal subfield of the hippocampal head (first row), body (second row), and tail (third row) are shown using ITK-SNAP software. The right two columns are the enlargement of the box in the left column. Abbreviations: DG, dentate gyrus; CA, Cornu Ammonis; Sub, subiculum; PHC, para-hippocampus; ERC, entorhinal cortex.

## RESULTS

### Data Characteristics

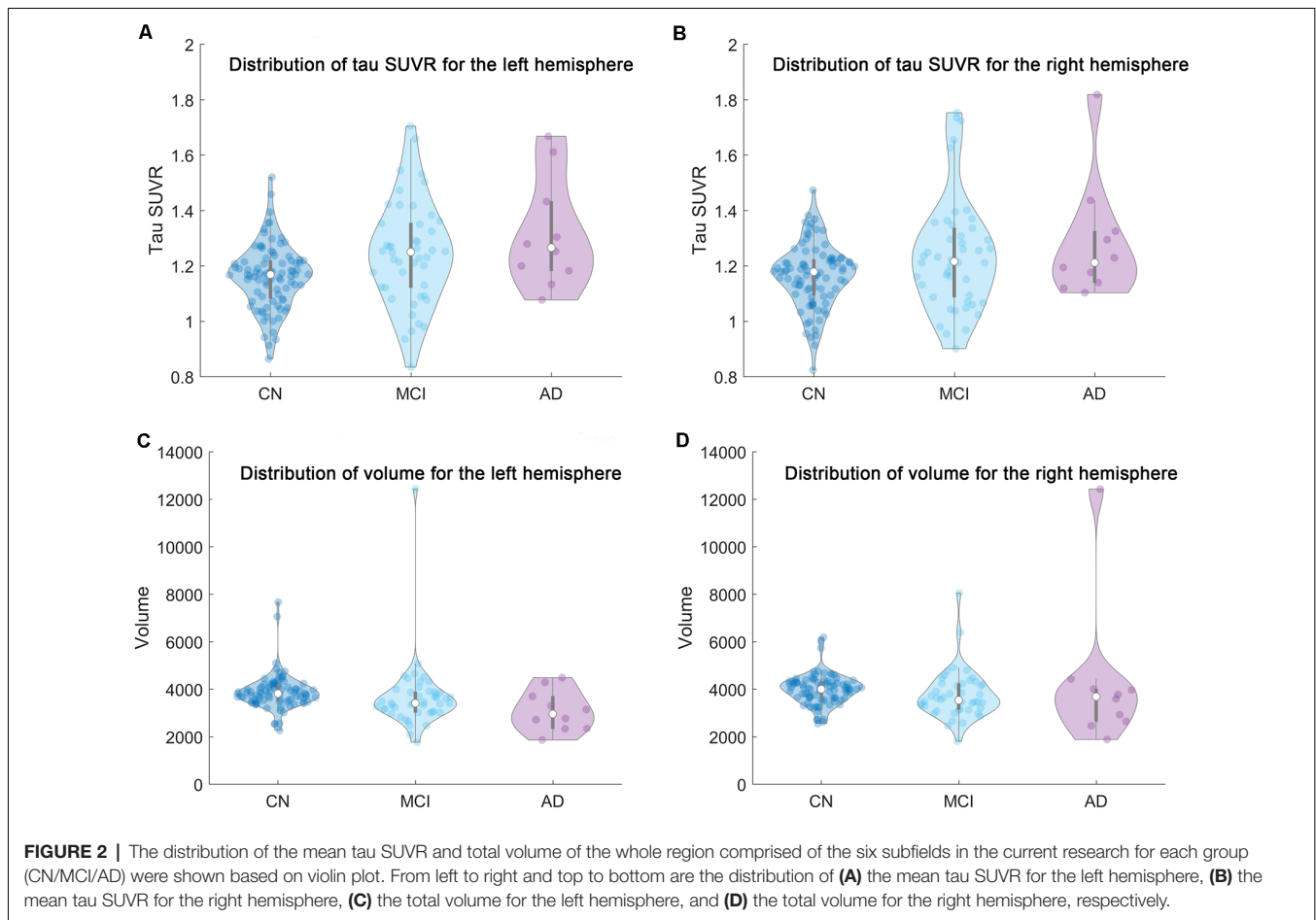
As we can see from **Table 1**, no significant difference in education level and gender distribution are found between the A– and A+ groups. Compared to the A– group, the A+ group has older subjects ( $p = 0.0192$ ), more *APOE* allele  $\epsilon 4$  carriers ( $p = 1.96e-06$ ), and is more impaired based on the MMSE ( $p = 3.82e-05$ ), memory ( $p = 6.30e-04$ ), executive function ( $p = 0.0016$ ), and ADAS-cog-13 scores ( $p = 5.11e-04$ ).

The distribution of the mean tau SUVR and total volume of the whole region comprised of the six subfields in the current study were plotted in **Figure 2**. We should note that there may be several outliers in the current cohort. Outliers were then removed from each group based on the mean tau SUVR and

total volume before the statistical analysis was conducted. If the outlier criterion was satisfied for any condition (mean SUVR or total volume for left or right hippocampi), this subject would be excluded as an outlier. These calculations were performed using the “isoutlier” function of MATLAB with the “mean” method. After outlier removal, three subjects in the amyloid negative group and one subject in the amyloid positive group were removed from the statistical analysis steps.

### Comparison of Volume and Tau Deposition of the Hippocampal Subfields Between Amyloid Negative and Positive Groups

Significant volume decreases of the CA1, Sub, and DG for both hemispheres are observed from the A– group to the A+ group.



Tau deposition of the CA1, Sub, ERC, and PHC for the A+ group increase significantly in both hemispheres compared to the A− group (Table 2).

### Hemispheric Differences of the Hippocampal Subfields Within Specific Amyloid Status

For A− group, no significant difference is found between the left and right hippocampal subfield for tau SUVR. Hemispheric differences were prominent for hippocampal volume (leftward lower) mainly in the CA1 ( $p = 0.0069$ ), DG ( $p = 0.0026$ ), PHC ( $p = 0.0026$ ), and CA2/CA3 ( $p = 1.92e-08$ ) regions.

Similarly, no significant difference is found between the left and right hippocampal subfield for tau SUVR within the A+ group. The hemispheric difference is also prominent for hippocampal volume (leftward lower) mainly in the PHC ( $p = 0.0055$ ) and CA2/CA3 ( $p = 2.57e-08$ ) regions.

### Partial Correlations Between Tau Deposition or Volume of the Hippocampal Subfields and Clinical Assessment Scores for A− Subjects

As can be seen from Table 3, the tau SUVR is found significantly correlated with memory score in the ERC for the left hemisphere,

while no significant correlation was observed between the other clinical scores and tau SUVR of the hippocampal subfields for either hemisphere.

Differently, the volume of the left Sub and CA1 are significantly correlated with memory score, while no significant correlation is observed between the other assessment scores and hippocampal volumes (Table 4).

### Partial Correlations Between Tau Deposition or Volume of the Hippocampal Subfields and Clinical Assessment Scores for A+ Subjects

As we can see from Table 5, significant correlations between the assessment scores and tau SUVR are found in the Sub, ERC, and PHC for the left hemisphere. Tau SUVR of CA1 region is also significantly associated with ADAS-cog-13 and NPI scores for the left hippocampi.

As to the right hemisphere, the correlations with tau SUVR are found in the ERC and the PHC with memory score, in the Sub, ERC, and PHC with ADAS-cog-13 score, and in the PHC with executive function score. No significant correlation is found between the NPI score and tau SUVR of the right hippocampal subfields.

**TABLE 2** | Volume and tau deposition of the hippocampal subfields between different amyloid status ( $p < 0.05$ , FDR correction. n.s.: not significant).

	Hemisphere	CA1	DG	Sub	ERC	PHC	CA2/CA3
Volume	Left	0.0036	0.0414	0.0414	n.s.	n.s.	n.s.
	Right	0.0037	0.0037	0.017	n.s.	n.s.	n.s.
SUVR	Left	0.0110	n.s.	0.0027	0.0001	0.0014	n.s.
	Right	0.0417	n.s.	0.0006	0.0001	0.0006	n.s.

**TABLE 3** | Associations between assessment scores and tau SUVR of the hippocampal subfields for A- group ( $p < 0.05$ , FDR correction).

Hemisphere	Assessment score	CA1	DG	Sub	ERC	PHC	CA2/CA3
Left	Memory	0.54	0.62	0.32	<b>0.04</b>	0.54	0.62
	ADAS-cog-13	0.49	0.49	0.18	0.18	0.35	0.49
	Executive function	0.47	0.47	0.47	0.47	0.47	0.47
	NPI	0.53	0.53	0.53	0.53	0.53	0.53
Right	Memory	0.67	0.81	0.52	0.051	0.67	0.81
	ADAS-cog-13	0.78	0.78	0.34	0.30	0.34	0.72
	Executive function	0.39	0.39	0.31	0.31	0.35	0.39
	NPI	0.30	0.30	0.30	0.30	0.30	0.30

Bold values mean the  $p$ 's  $< 0.05$  and statistically significant.

**TABLE 4** | Associations between assessment scores and volume of the hippocampal subfields for A- group ( $p < 0.05$ , FDR correction).

Hemisphere	Assessment score	CA1	DG	Sub	ERC	PHC	CA2/CA3
Left	Memory	<b>0.01</b>	0.053	<b>0.004</b>	0.16	0.96	0.96
	ADAS-cog-13	0.07	0.43	0.07	0.61	0.96	0.48
	Executive function	0.50	0.86	0.09	0.86	0.86	0.48
	NPI	0.92	0.92	0.88	0.92	0.56	0.92
Right	Memory	0.27	0.21	0.21	0.21	0.31	0.78
	ADAS-cog-13	0.55	0.55	0.55	0.55	0.89	0.55
	Executive function	0.99	0.96	0.39	0.39	0.39	0.99
	NPI	0.51	0.51	0.51	0.67	0.51	0.67

Bold values mean the  $p$ 's  $< 0.05$  and statistically significant.

**TABLE 5** | Associations between assessment scores and tau SUVR of the hippocampal subfields for A+ group ( $p < 0.05$ , FDR correction).

Hemisphere	Assessment score	CA1	DG	Sub	ERC	PHC	CA2/CA3
Left	Memory	0.08	0.64	<b>0.01</b>	<b>0.003</b>	<b>0.003</b>	0.20
	ADAS-cog-13	<b>0.02</b>	0.31	<b>0.001</b>	<b>0.0005</b>	<b>0.0005</b>	0.72
	Executive function	0.37	0.90	<b>0.048</b>	<b>0.008</b>	<b>0.008</b>	0.51
	NPI	<b>0.04</b>	0.25	<b>0.03</b>	<b>0.03</b>	<b>0.03</b>	0.83
Right	Memory	0.26	0.74	0.059	<b>0.03</b>	<b>0.02</b>	0.45
	ADAS-cog-13	0.06	0.51	<b>0.004</b>	<b>0.002</b>	<b>0.009</b>	0.84
	Executive function	0.43	0.74	0.11	0.054	<b>0.03</b>	0.74
	NPI	0.20	0.27	0.20	0.27	0.20	0.82

Bold values mean the  $p$ 's  $< 0.05$  and statistically significant.

**TABLE 6** | Associations between assessment scores and volume of the hippocampal subfields for A+ group ( $p < 0.05$ , FDR correction).

Hemisphere	Assessment score	CA1	DG	Sub	ERC	PHC	CA2/CA3
Left	Memory	<b>0.008</b>	<b>0.008</b>	<b>0.03</b>	<b>0.008</b>	<b>0.02</b>	<b>0.04</b>
	ADAS_cog_13	0.14	0.23	0.11	0.11	0.74	0.68
	Executive function	0.16	0.12	0.19	0.35	0.12	0.83
	NPI	<b>0.008</b>	<b>0.008</b>	0.06	<b>0.005</b>	0.25	<b>0.008</b>
Right	Memory	<b>0.04</b>	0.053	0.053	<b>0.0004</b>	0.39	<b>0.04</b>
	ADAS_cog_13	0.09	0.17	0.09	<b>0.02</b>	0.91	0.15
	Executive function	0.10	<b>0.03</b>	0.12	<b>0.03</b>	0.12	0.12
	NPI	<b>0.07</b>	0.12	<b>0.01</b>	<b>0.003</b>	0.39	0.06

Bold values mean the  $p$ 's  $< 0.05$  and statistically significant.

Significant correlations between the volumes and memory score are found in all the subfields for the left hemisphere, while the association is only found with the CA1, ERC, and

CA2/CA3 regions for the right hippocampi. The volume of the CA1, DG, ERC, and CA2/CA3 are found significantly correlated with the NPI score for the left hemisphere. However, there

is no significant correlation between the volume of the left subfields with either ADAS\_cog\_13 or executive function score. Differently, the ADAS\_cog\_13 score is found to be significantly correlated with the volume of the ERC and the executive function score is significantly correlated with the volume of the DG and ERC for the right hemisphere. The NPI total score is found associated with the volume of the CA1, Sub, and ERC for the right hippocampi (**Table 6**).

## DISCUSSION

Atrophy of the HF is one of the early biomarkers for the diagnosis of neurodegenerative disorders including AD (Pizzi et al., 2016). However, neurodegeneration such as changes of the HF is not specific to AD and several neuropsychiatric disorders may have the same outcomes (Das et al., 2019). With the proposed AT[N] framework, the combination of the neurodegeneration assessed by the decrease of cortical thickness or the atrophy of HF and AD-related biomarkers such as pathology of amyloid and tau proteins were used to distinguish the stages of the AD continuum (Jack et al., 2016). In the current study, the memory score was found significantly associated with tau pathology in the ERC of the left hemisphere compared to the other hippocampal subfields, even for the amyloid negative individuals. On the contrary, impairment of cognition, behavior, and executive function were related to the changes of tauopathy/volume of hippocampal subfields when the amyloid status became positive. The impairment patterns of the hippocampal subfields observed in the current research are essential for the understanding of the AD spectrum and can be used as a reference for future AD studies.

Pathology of amyloid and tau proteins are the two defining hallmarks that can characterize the progression of AD. The presence of abnormal amyloid status was regarded as the 'disease state' to determine if the subject is during the Alzheimer's pathologic process (Brier et al., 2016). Individuals with positive amyloid biomarkers demonstrated a higher risk of the conversion from cognitive normal to mild cognitive impairment (Donohue et al., 2017). There is a strong association of elevated tau deposition in both medial temporal lobe structures and the neocortex with positive amyloid status across the normal aging to clinical dementia (Marks et al., 2017). In the current study, higher tau deposition is discovered in the CA1, Sub, ERC, and PHC of both hemispheres for the A+ group as compared to the A- group (**Table 2**). Significant volume decreases of the CA1, DG, and Sub of both hemispheres are also observed from the A- group to the A+ group. All confirm the increased disease severity with the presence of elevated amyloid pathology.

Previous studies showed that tau pathology in the medial temporal lobe (MTL) is a key driver of memory impairment in AD and is an important biomarker for neurodegeneration (Marks et al., 2017; Scott et al., 2020). Repeated tau PET scans have been an effective measurement to track the disease progression, while amyloid PET is more responsible for the detection of the early Alzheimer pathology (Hanseeuw et al., 2019). Tau deposition in the temporal lobe has been a better

predictor of cognitive decline than the emergence of amyloid plaques in any region of the brain (Brier et al., 2016). The crucial role of tau deposition is recommended as a candidate target for AD therapy to deal with the limitations of the amyloid cascade hypothesis (Giacobini and Gold, 2013). We thus focused on the association of tau pathology with clinical symptoms in the hippocampal subfields under different amyloid statuses to delineate the detailed progression of AD. Tau SUVR of the ERC showed a significant correlation with the comprised memory score for the A- subjects in the current research (**Table 3**). ERC is one of the most vulnerable regions for the deposition of tau tangles and is closely associated with memory function (Braak et al., 2011). Impairment of the ERC has been regarded as an essential marker for the classical analysis of AD. Our results confirmed that the ERC should be paid more attention for the subsequent studies.

With the presence of amyloid pathology, the correlation between the tau SUVR with assessment scores spread into several subfields (**Table 5**). The tau SUVR of the Sub, ERC, and PHC are correlated with the comprised memory score, ADAS-cog-13 score, executive function score, and NPI total score for the left hippocampi. The tau SUVR of the CA1 region is also found significantly associated with the ADAS-cog-13 score and NPI total score for the left hemisphere. For the right hippocampi, the comprised memory score and ADAS-cog-13 score are found significantly correlated with the deposition of tau tangles in the ERC and PHC. It is known that the spatiotemporal spread of tau tangles follows a stereotypical trajectory starting from the locus coeruleus and the trans-entorhinal cortex, and then extending to the ERC, the HF, and finally the neocortex (Fuster-Matanzo et al., 2018). The associations between the tau deposition of the hippocampal subfields and assessment scores in the current research demonstrate that the development of AD may be affected in a progressive manner from the ERC and the PHC to the Sub, and eventually to the CA1 region on a smaller scale. On the other hand, the DG and the CA2/CA3 regions are less affected by the tau pathology. The DG is one of the few areas in the mammalian brain in which new excitatory neurons are continuously generated throughout life. The neural plasticity that results from the continuous integration of newly born excitatory granule cells may contribute to the DG network activity and withstand tau deposition. This could finally slow the disease progression (Tuncdemir et al., 2019; Christian et al., 2020). In addition, the NPI total score and executive function score were only found correlated with tau SUVR or volume of the hippocampal subfields with the presence of elevated amyloid pathology, which indicates that the decline of behavior and executive function is consistent with the neurodegenerative alterations of the HF when the subject was in the Alzheimer's pathologic process.

Volume changes of the hippocampal subfields are not as regular as the deposition of tau tangles. The CA1, DG, and Sub of both hemispheres have a volume decrease in the A+ group as compared to the A- group, while no significant difference is found in the ERC, PHC, and CA2/CA3 (**Table 2**). There is nearly no significant association between the volume

of the hippocampal subfields and assessment scores (except for the memory score) for the A- subjects (Table 4). With the presence of amyloid pathology, the relationship between the volume of the hippocampal subfields and assessment score is in conformity (Table 6). One possibility is that the volumetric changes of the hippocampal subfields are the sum of influences from normal aging and diverse neurodegenerative disorders such as AD, PD, and depression (Knopman et al., 2019). Individuals with diverse neuropsychiatric disorders may also be diagnosed as MCI or AD, which may affect the statistical results in the current study. Using volume changes of brain region without the help of AD-specific biomarkers is insufficient for the accurate diagnosis of AD (Edmonds et al., 2016; Sørensen et al., 2017).

Hemispheric difference is a classic topic in the neuroimaging area and still possesses a vital debate (Toga and Thompson, 2003; Pedraza et al., 2004; Woolard and Heckers, 2012). The left hippocampus was found more impaired than the right for individuals with subjective cognitive decline (Yue et al., 2018), as well as for the MCI and AD subjects (Shi et al., 2009). Similar results are discovered in the current research with the CA1 ( $p = 0.0069$ ), DG ( $p = 0.0026$ ), PHC ( $p = 0.0026$ ), and CA2/CA3 ( $p = 1.92e-08$ ) regions showing lower volume for the A- individuals. Lower volume of the left PHC ( $p = 0.0055$ ) and CA2/CA3 ( $p = 2.57e-08$ ) regions are also found for A+ group. In addition, the asymmetry of the association patterns between the tau SUVR of the hippocampal subfields and the assessment scores are obviously observed, and particularly more prominent for the NPI total score with the presence of elevated amyloid pathology (Table 5). Behavior symptoms including apathy, anxiety, and sleeping problems may be related to diverse brain functions and changes of specific hippocampal subfields (Chen et al., 2018; Campabadal et al., 2019; Dalton et al., 2019). The leftward asymmetry in the current research shows that the progression of AD may seriously affect the left hippocampi as compared to the right hemisphere.

## LIMITATIONS

The diagnosis of the patients from ADNI is based on the clinical symptoms and clinical assessment scores other than the amyloid PET or tau PET scans. This is why one AD patient and some MCI individuals are included in the A- group, while many CN subjects are found in the A+ groups. Considering the integrity of the original data as well as the relatively small sample size, we put the CN, MCI, and AD subjects together for the statistical analysis in the current study. It is insufficient to observe the alterations of tau deposition or volume changes of the hippocampal subfields during a specific stage of AD (normal aging, mild cognitive impairment, or AD) based on the limited data. This is one of the reasons why the association between the volume of hippocampal subfields and assessment scores show no consistent patterns as compared to the tau deposition. In addition, there is a significant difference of age between the A- and A+ groups (Table 1). However, the influence of normal aging is not demonstrated thoroughly even if we considered age as a covariance in the partial

correlation process. On the other hand, NPI has 12 domains to assess the behavior symptoms of each subject and is widely used for the assessment of treatment effect (Cummings, 1997). However, the sample size of the current study is insufficient for the analysis of one specific behavior domain. Further analysis focused on the cohort with the same clinical diagnosis, as well as with the matched distribution of age, gender, education, etc., should be conducted with the development of the ADNI project.

Another limitation is that the relatively low resolution of the PET images may influence the calculation of the tau deposition for each hippocampal subfield. No partial volume correction was performed in this study, which may introduce signal mixture to small brain regions (Brendel et al., 2015; Matsubara et al., 2016; Rullmann et al., 2016; Su et al., 2016; Baker et al., 2017; Gonzalez-Escamilla et al., 2017). This is one of the reasons why the CA2 and CA3 were considered together and relatively large regions such as the CA1, ERC, and PHC were considered in the statistical analysis.

Not enough longitudinal data of the high-resolution T2 weighted MR images and tau PET scans for the statistical analysis were acquired based on the current inclusion criteria. AD is a neurodegenerative disorder that may go through several decades before clinical diagnosis. Observation of the dynamic changes of the tau deposition of the hippocampal subfields and its association with assessment scores in the future is essential for the early diagnosis and prevention of AD dementia.

## CONCLUSION

The current research has found that the development of AD may be affected in a progressive manner from the ERC to the PHC, the Sub, and eventually to the CA1 region on a smaller scale. The relationship between the clinical symptoms and tauopathy/volume of the hippocampal subfield showed diverse patterns under different amyloid statuses. Leftward asymmetry was observed with the association between assessment scores and tauopathy/volume of the hippocampal subfield, which is more prominent for the NPI total score in the current study. The associations of tauopathy/volume of the hippocampal subfields with the clinical symptoms are essential for the understanding of the AD spectrum and can be used as the reference for future AD studies.

## DATA AVAILABILITY STATEMENT

The datasets presented in this study can be found in online repositories. The names of the repository/repositories and accession number(s) can be found in the article.

## ETHICS STATEMENT

Written informed consent was obtained from the individual(s) for the publication of any potentially identifiable images or data included in this article.

## AUTHOR CONTRIBUTIONS

XG wrote the first draft of the manuscript. YZ and JX contributed to conception and design of the study. YQ and JZ performed the statistical analysis. XG and DZ organized the database and designed the protocol. All authors contributed to the article and approved the submitted version.

## FUNDING

This work was supported by the National Natural Science Foundation of China (No. 81801776), Natural Science Foundation of Jiangsu Province (No. BK20170256), and Science and Technology Development Program of Xuzhou (No. KC17164). The work of JX was supported by the Project funded by China: Postdoctoral Science Foundation (2020M680905).

## ACKNOWLEDGMENTS

Data collection and sharing for this project was funded by the Alzheimer's Disease Neuroimaging Initiative (ADNI) (National Institutes of Health Grant U01 AG024904) and DOD ADNI (Department of Defense award number W81XWH-12-2-0012).

## REFERENCES

- Adler, D. H., Wisse, L. E., Ittyerah, R., Pluta, J. B., Ding, S.-L., Xie, L., et al. (2018). Characterizing the human hippocampus in aging and Alzheimer's disease using a computational atlas derived from *ex vivo* MRI and histology. *Proc. Natl. Acad. Sci. U S A* 115, 4252–4257. doi: 10.1073/pnas.1801093115
- Baker, S. L., Maass, A., and Jagust, W. J. (2017). Considerations and code for partial volume correcting [18F]-AV-1451 tau PET data. *Data Brief* 15, 648–657. doi: 10.1016/j.dib.2017.10.024
- Braak, H., and Del Tredici, K. (2011). Alzheimer's pathogenesis: is there neuron-to-neuron propagation. *Acta Neuropathol.* 121, 589–595. doi: 10.1007/s00401-011-0825-z
- Braak, H., Thal, D. R., Ghebremedhin, E., and Del Tredici, K. (2011). Stages of the pathologic process in Alzheimer disease: age categories from 1 to 100 years. *J. Neuropathol. Exp. Neurol.* 70, 960–969. doi: 10.1097/NEN.0b013e318232a379
- Brendel, M., Högenauer, M., Delker, A., Sauerbeck, J., Bartenstein, P., Seibyl, J., et al. (2015). Improved longitudinal [18F]-AV45 amyloid PET by white matter reference and VOI-based partial volume effect correction. *NeuroImage* 108, 450–459. doi: 10.1016/j.neuroimage.2014.11.055
- Brier, M. R., Gordon, B., Friedrichsen, K., McCarthy, J., Stern, A., Christensen, J., et al. (2016). Tau and A $\beta$  imaging, CSF measures and cognition in Alzheimer's disease. *Sci. Transl. Med.* 8:338ra366. doi: 10.1126/scitranslmed.aaf2362
- Campabadal, A., Segura, B., Junque, C., Serradell, M., Abos, A., Uribe, C., et al. (2019). Cortical gray matter and hippocampal atrophy in idiopathic Rapid Eye Movement sleep behavior disorder. *Front. Neurol.* 10:312. doi: 10.3389/fneur.2019.00312
- Chen, L. W., Sun, D., Davis, S. L., Haswell, C. C., Dennis, E. L., Swanson, C. A., et al. (2018). Smaller hippocampal CA1 subfield volume in posttraumatic stress disorder. *Depress. Anxiety* 35, 1018–1029. doi: 10.1002/da.22833
- Christian, K. M., Ming, G.-L., and Song, H. (2020). Adult neurogenesis and the dentate gyrus: predicting function from form. *Behav. Brain Res.* 379:112346. doi: 10.1016/j.bbr.2019.112346
- Cummings, J. L. (1997). The neuropsychiatric inventory: assessing psychopathology in dementia patients. *Neurology* 48, S10–S16. doi: 10.1212/wnl.48.5\_suppl\_6.10s
- ADNI is funded by the National Institute on Aging, the National Institute of Biomedical Imaging and Bioengineering, and through generous contributions from the following: AbbVie, Alzheimer's Association; Alzheimer's Drug Discovery Foundation; Araclon Biotech; BioClinica, Inc.; Biogen; Bristol-Myers Squibb Company; CereSpir, Inc.; Cogstate; Eisai Inc.; Elan Pharmaceuticals, Inc.; Eli Lilly and Company; EuroImmun; F. Hoffmann-La Roche Ltd. and its affiliated company Genentech, Inc.; Fujirebio; GE Healthcare; IXICO Ltd.; Janssen Alzheimer Immunotherapy Research & Development, LLC.; Johnson & Johnson Pharmaceutical Research & Development LLC.; Lumosity; Lundbeck; Merck & Co., Inc.; Meso Scale Diagnostics, LLC.; NeuroRx Research; Neurotrack Technologies; Novartis Pharmaceuticals Corporation; Pfizer Inc.; Piramal Imaging; Servier; Takeda Pharmaceutical Company; and Transition Therapeutics. The Canadian Institutes of Health Research is providing funds to support ADNI clinical sites in Canada. Private sector contributions are facilitated by the Foundation for the National Institutes of Health ([www.fnih.org](http://www.fnih.org)). The grantee organization is the Northern California Institute for Research and Education, and the study is coordinated by the Alzheimer's Therapeutic Research Institute at the University of Southern California. ADNI data are disseminated by the Laboratory for Neuro Imaging at the University of Southern California.
- Dalton, M. A., McCormick, C., and Maguire, E. A. (2019). Differences in functional connectivity along the anterior-posterior axis of human hippocampal subfields. *NeuroImage* 192, 38–51. doi: 10.1016/j.neuroimage.2019.02.066
- Das, T., Hwang, J. J., and Poston, K. L. (2019). Episodic recognition memory and the hippocampus in Parkinson's disease: a review. *Cortex* 113, 191–209. doi: 10.1016/j.cortex.2018.11.021
- Deb, A., Sambamoorthi, U., Thornton, J. D., Schreurs, B., Innes, K. J. A., and health, M. (2018). Direct medical expenditures associated with Alzheimer's and related dementias (ADRD) in a nationally representative sample of older adults—an excess cost approach. *Aging Ment. Health* 22, 619–624. doi: 10.1080/13607863.2017.1286454
- Desikan, R. S., Ségonne, F., Fischl, B., Quinn, B. T., Dickerson, B. C., Blacker, D., et al. (2006). An automated labeling system for subdividing the human cerebral cortex on MRI scans into gyral based regions of interest. *NeuroImage* 31, 968–980. doi: 10.1016/j.neuroimage.2006.01.021
- Donohue, M. C., Sperling, R. A., Petersen, R., Sun, C.-K., Weiner, M. W., and Aisen, P. S. J. J. (2017). Association between elevated brain amyloid and subsequent cognitive decline among cognitively normal persons. *JAMA* 317, 2305–2316. doi: 10.1001/jama.2017.6669
- Edmonds, E. C., Eppig, J., Bondi, M. W., Leyden, K. M., Goodwin, B., Delano-Wood, L., et al. (2016). Heterogeneous cortical atrophy patterns in MCI not captured by conventional diagnostic criteria. *Neurology* 87, 2108–2116. doi: 10.1212/WNL.00000000000003326
- Evans, T. E., Adams, H. H., Licher, S., Wolters, F. J., van der Lugt, A., Ikram, M. K., et al. (2018). Subregional volumes of the hippocampus in relation to cognitive function and risk of dementia. *NeuroImage* 178, 129–135. doi: 10.1016/j.neuroimage.2018.05.041
- Fuster-Matanzo, A., Hernández, F., and Ávila, J. (2018). Tau spreading mechanisms; implications for dysfunctional tauopathies. *Int. J. Mol. Sci.* 19:645. doi: 10.3390/ijms19030645
- Giacobini, E., and Gold, G. (2013). Alzheimer disease therapy—moving from amyloid- $\beta$  to tau. *Nat. Rev. Neurol.* 9, 677–686. doi: 10.1038/nrneurol.2013.223

- Gonzalez-Escamilla, G., Lange, C., Teipel, S., Buchert, R., Grothe, M. J., and Initiative, A. S. D. N. (2017). PETPVE12: an SPM toolbox for partial volume effects correction in brain PET-application to amyloid imaging with AV45-PET. *NeuroImage* 147, 669–677. doi: 10.1016/j.neuroimage.2016.12.077
- Gordon, B. A., Blazey, T. M., Christensen, J., Dincer, A., Flores, S., Keefe, S., et al. (2019). Tau PET in autosomal dominant Alzheimer's disease: relationship with cognition, dementia and other biomarkers. *Brain* 142, 1063–1076. doi: 10.1093/brain/awz019
- Hanseeuw, B. J., Betensky, R. A., Jacobs, H. I., Schultz, A. P., Sepulcre, J., Becker, J. A., et al. (2019). Association of amyloid and tau with cognition in preclinical Alzheimer disease: a longitudinal study. *JAMA Neurol.* 76, 915–924. doi: 10.1001/jamaneurol.2019.1424
- Ikram, M. A., Vrooman, H. A., Vernooij, M. W., den Heijer, T., Hofman, A., Niessen, W. J., et al. (2010). Brain tissue volumes in relation to cognitive function and risk of dementia. *Neurobiol. Aging* 31, 378–386. doi: 10.1016/j.neurobiolaging.2008.04.008
- Ismail, Z., Smith, E. E., Geda, Y., Sultzer, D., Brodaty, H., Smith, G., et al. (2016). Neuropsychiatric symptoms as early manifestations of emergent dementia: provisional diagnostic criteria for mild behavioral impairment. *JAMA Neurol.* 12, 195–202. doi: 10.1016/j.jalz.2015.05.017
- Jack Jr, C. R., Bennett, D. A., Blennow, K., Carrillo, M. C., Dunn, B., Haeblerlein, S. B., et al. (2018). NIA-AA research framework: toward a biological definition of Alzheimer's disease. *Alzheimers Dement.* 14, 535–562. doi: 10.1016/j.jalz.2018.02.018
- Jack, C. R., Bennett, D. A., Blennow, K., Carrillo, M. C., Feldman, H. H., Frisoni, G. B., et al. (2016). A/T/N: an unbiased descriptive classification scheme for Alzheimer disease biomarkers. *Neurology* 87, 539–547. doi: 10.1212/WNL.0000000000002923
- Jack, C. R., Wiste, H. J., Therneau, T. M., Weigand, S. D., Knopman, D. S., Mielke, M. M., et al. (2019). Associations of amyloid, tau and neurodegeneration biomarker profiles with rates of memory decline among individuals without dementia. *JAMA* 321, 2316–2325. doi: 10.1001/jama.2019.7437
- Knopman, D. S., Lundt, E. S., Therneau, T. M., Vemuri, P., Lowe, V. J., Kantarci, K., et al. (2019). Entorhinal cortex tau, amyloid- $\beta$ , cortical thickness and memory performance in non-demented subjects. *Brain* 142, 1148–1160. doi: 10.1093/brain/awz025
- Kueper, J. K., Speechley, M., and Montero-Odasso, M. (2018). The Alzheimer's disease assessment scale-cognitive subscale (ADAS-Cog): modifications and responsiveness in pre-dementia populations. a narrative review. *J. Alzheimer's Dis.* 63, 423–444. doi: 10.3233/JAD-170991
- Landau, S., Thomas, B., Thurfjell, L., Schmidt, M., Margolin, R., Mintun, M., et al. (2014). Amyloid PET imaging in Alzheimer's disease: a comparison of three radiotracers. *Eur. J. Nucl. Med. Mol. Imaging* 41, 1398–1407. doi: 10.1007/s00259-014-2753-3
- Marks, S. M., Lockhart, S. N., Baker, S. L., and Jagust, W. J. (2017). Tau and  $\beta$ -amyloid are associated with medial temporal lobe structure, function and memory encoding in normal aging. *J. Neurosci.* 37, 3192–3201. doi: 10.1523/JNEUROSCI.3769-16.2017
- Masters, M. C., Morris, J. C., and Roe, C. M. J. N. (2015). "Noncognitive" symptoms of early Alzheimer disease: a longitudinal analysis. *Neurology* 84, 617–622. doi: 10.1212/WNL.0000000000001238
- Matsubara, K., Ibaraki, M., Shimada, H., Ikoma, Y., Suhara, T., Kinoshita, T., et al. (2016). Impact of spillover from white matter by partial volume effect on quantification of amyloid deposition with [ $^{11}\text{C}$ ] PiB PET. *NeuroImage* 143, 316–324. doi: 10.1016/j.neuroimage.2016.09.028
- McCartney, D. L., Stevenson, A. J., Walker, R. M., Gibson, J., Morris, S. W., Campbell, A., et al. (2018). Investigating the relationship between DNA methylation age acceleration and risk factors for Alzheimer's disease. *Alzheimers Dement. (Amst).* 10, 429–437. doi: 10.1016/j.dadm.2018.05.006
- Mok, W. Y., Chu, L., Chung, C., Chan, N., and Hui, S. L. (2004). The relationship between non-cognitive symptoms and functional impairment in Alzheimer's disease. *Int. J. Geriatr. Psychiatry* 19, 1040–1046. doi: 10.1002/gps.1207
- Moreno-Jiménez, E. P., Flor-García, M., Terreros-Roncal, J., Rábano, A., Cafini, F., Pallas-Bazarrá, N., et al. (2019). Adult hippocampal neurogenesis is abundant in neurologically healthy subjects and drops sharply in patients with Alzheimer's disease. *Nat. Med.* 25, 554–560. doi: 10.1038/s41591-019-0375-9
- Naidich, T., Daniels, D., Haughton, V., Williams, A., Pojunas, K., and Palacios, E. (1987). Hippocampal formation and related structures of the limbic lobe: anatomic-MR correlation. Part I. Surface features and coronal sections. *Radiology* 162, 747–754. doi: 10.1148/radiology.162.3.3809489
- Nunes, P. V., Schwarzer, M. C., Leite, R. E. P., Ferretti-Rebustini, R. E. L., Pasqualucci, C. A., Nitrini, R., et al. (2019). Neuropsychiatric inventory in community-dwelling older adults with mild cognitive impairment and dementia. *J. Alzheimers Dis.* 68, 669–678. doi: 10.3233/JAD-180641
- Parker, T. D., Slattery, C. F., Yong, K. X., Nicholas, J. M., Paterson, R. W., Foulkes, A. J., et al. (2019). Differences in hippocampal subfield volume are seen in phenotypic variants of early onset Alzheimer's disease. *Neuroimage Clin.* 21:101632. doi: 10.1016/j.nicl.2018.101632
- Pedraza, O., Bowers, D., and Gilmore, R. (2004). Asymmetry of the hippocampus and amygdala in MRI volumetric measurements of normal adults. *J. Int. Neuropsychol. Soc.* 10, 664–678. doi: 10.1017/S1355617704105080
- Petersen, R. C., Aisen, P., Beckett, L. A., Donohue, M., Gamst, A., Harvey, D. J., et al. (2010). Alzheimer's disease neuroimaging initiative (ADNI): clinical characterization. *Neurology* 74, 201–209. doi: 10.1212/WNL.0b013e3181cb3e25
- Pizzi, S. D., Franciotti, R., Bubbico, G., Thomas, A., Onofri, M., and Bonanni, L. (2016). Atrophy of hippocampal subfields and adjacent extrahippocampal structures in dementia with Lewy bodies and Alzheimer's disease. *Neurobiol. Aging* 40, 103–109. doi: 10.1016/j.neurobiolaging.2016.01.010
- Rullmann, M., Dukart, J., Hoffmann, K.-T., Luthardt, J., Tiegelt, S., Patt, M., et al. (2016). Partial-volume effect correction improves quantitative analysis of 18F-florbetaben  $\beta$ -amyloid PET scans. *J. Nucl. Med.* 57, 198–203. doi: 10.2967/jnumed.115.161893
- Scharre, D. W. (2019). Preclinical, prodromal and dementia stages of Alzheimer's disease. *Pract. Neurol.* Available online at: <https://practicalneurology.com/articles/2019-june/preclinical-prodromal-and-dementia-stages-of-alzheimers-disease/pdf>.
- Scott, M. R., Hampton, O. L., Buckley, R. F., Chhatwal, J. P., Hanseeuw, B. J., Jacobs, H. I., et al. (2020). Inferior temporal tau is associated with accelerated prospective cortical thinning in clinically normal older adults. *NeuroImage* 220:116991. doi: 10.1016/j.neuroimage.2020.116991
- Shi, F., Liu, B., Zhou, Y., Yu, C., and Jiang, T. (2009). Hippocampal volume and asymmetry in mild cognitive impairment and Alzheimer's disease: meta-analyses of MRI studies. *Hippocampus* 19, 1055–1064. doi: 10.1002/hipo.20573
- Sørensen, L., Igel, C., Pai, A., Balas, I., Anker, C., Lillholm, M., et al. (2017). Differential diagnosis of mild cognitive impairment and Alzheimer's disease using structural MRI cortical thickness, hippocampal shape, hippocampal texture and volumetry. *Neuroimage Clin.* 13, 470–482. doi: 10.1016/j.nicl.2016.11.025
- Su, Y., Blazey, T. M., Owen, C. J., Christensen, J. J., Friedrichsen, K., Joseph-Mathurin, N., et al. (2016). Quantitative amyloid imaging in autosomal dominant Alzheimer's disease: results from the DIAN study group. *PLoS One* 11:e0152082. doi: 10.1371/journal.pone.0152082
- Toga, A. W., and Thompson, P. M. (2003). Mapping brain asymmetry. *Nat. Rev. Neurosci.* 4, 37–48. doi: 10.1038/nrn1009
- Tosun, D., Landau, S., Aisen, P. S., Petersen, R. C., Mintun, M., Jagust, W., et al. (2017). Association between tau deposition and antecedent amyloid-beta accumulation rates in normal and early symptomatic individuals. *Brain* 140, 1499–1512. doi: 10.1093/brain/awx046
- Tuncdemir, S. N., Lacefield, C. O., and Hen, R. (2019). Contributions of adult neurogenesis to dentate gyrus network activity and computations. *Behav. Brain Res.* 374:112112. doi: 10.1016/j.bbr.2019.112112
- Weiner, M. W., Veitch, D. P., Aisen, P. S., Beckett, L. A., Cairns, N. J., Cedarbaum, J., et al. (2015). 2014 Update of the Alzheimer's Disease Neuroimaging Initiative: a review of papers published since its inception. *Alzheimers Dement.* 11, e1–e120. doi: 10.1016/j.jalz.2014.11.001
- Woolard, A. A., and Heckers, S. (2012). Anatomical and functional correlates of human hippocampal volume asymmetry. *Psychiatry Res.* 201, 48–53. doi: 10.1016/j.psychres.2011.07.016
- Yoon, E. J., Ismail, Z., Hanganu, A., Kibreab, M., Hammer, T., Cheetham, J., et al. (2019). Mild behavioral impairment is linked to worse cognition and brain

- atrophy in Parkinson disease. *Neurology* 93, e766–e777. doi: 10.1212/WNL.0000000000007968
- Yue, L., Wang, T., Wang, J., Li, G., Wang, J., Li, X., et al. (2018). Asymmetry of hippocampus and amygdala defect in subjective cognitive decline among the community dwelling chinese. *Front. Psychiatry* 9:226. doi: 10.3389/fpsy.2018.00226
- Yushkevich, P. A., Pluta, J. B., Wang, H., Xie, L., Ding, S.-L., Gertje, E. C., et al. (2015). Automated volumetry and regional thickness analysis of hippocampal subfields and medial temporal cortical structures in mild cognitive impairment. *Hum. Brain Mapp.* 36, 258–287. doi: 10.1002/hbm.22627
- Zhao, Q.-F., Tan, L., Wang, H.-F., Jiang, T., Tan, M.-S., Tan, L., et al. (2016). The prevalence of neuropsychiatric symptoms in Alzheimer's disease: systematic review and meta-analysis. *J. Affect. Disord.* 190, 264–271. doi: 10.1016/j.jad.2015.09.069
- Zhao, W., Wang, X., Yin, C., He, M., Li, S., and Han, Y. (2019). Trajectories of the hippocampal subfields atrophy in the Alzheimer's disease: a structural imaging study. *Front. Neuroinform.* 13:13. doi: 10.3389/fninf.2019.00013

**Conflict of Interest:** The authors declare that the research was conducted in the absence of any commercial or financial relationships that could be construed as a potential conflict of interest.

Copyright © 2021 Ge, Zhang, Qiao, Zhang, Xu and Zheng. This is an open-access article distributed under the terms of the Creative Commons Attribution License (CC BY). The use, distribution or reproduction in other forums is permitted, provided the original author(s) and the copyright owner(s) are credited and that the original publication in this journal is cited, in accordance with accepted academic practice. No use, distribution or reproduction is permitted which does not comply with these terms.